Light emission from surface plasmon polaritons mediated by metallic fine particles

T. Kume
Division of Science of Materials, The Graduate School of Science and Technology, Kobe University, Rokkodai, Nada, Kobe 657, Japan

S. Hayashi* and K. Yamamoto
Division of Science of Materials, The Graduate School of Science and Technology and Department of Electrical and Electronics Engineering, Faculty of Engineering, Kobe University, Rokkodai, Nada, Kobe 657, Japan

(Received 6 September 1996)

A system of Ag nanoparticles placed very close to an Al surface was prepared by depositing an Ag-SiO_2 composite film on an Al film. Surface plasmon polaritons (SPP's) on the Al surface were excited by an attenuated total reflection (ATR) method and light emission from the SPP's caused by the presence of the Ag nanoparticles was measured. The intensity of emitted light was found to rapidly decrease as the distance between the particles and the surface increases. From a good qualitative agreement between experimental results and those of electromagnetic calculations, the following processes of light emission are suggested: (i) The SPP's excited by the ATR method excite the electromagnetic normal modes localized in between the Ag particles and the Al surface (gap modes), (ii) the gap modes then induce localized surface current on the Al surface, and (iii) the induced surface current emits light. [S0163-1829(97)07507-3]

I. INTRODUCTION

A system consisting of a metallic particle placed close to a metallic flat surface has been the subject of intensive experimental and theoretical studies for a relatively long time. The electromagnetic interaction between the particle and the surface is known to cause various interesting optical phenomena. McCarthy and Lambe[1] reported that metallic small particles deposited on a metal-insulator-metal tunnel junction lead to an enhancement of the light emission driven by a tunnel current. According to electromagnetic theories,[2–5] there exists a special type of electromagnetic normal mode (called the gap mode) localized in a space between the sphere and the surface. The gap mode is considered to be a source of the light emission from the tunnel junctions.[2,3] The contribution of the gap mode excited by a tunnel current was also pointed out for the light emission from a metal tip-metal surface system, i.e., a scanning tunneling microscope.[6–9]

Several attempts have been made recently to use the interaction between the metal tip and the metal surface in scanning near-field optical microscopy (SNOM).[10–13] Specht *et al.*[11] demonstrated a different type of SNOM, which is based on the interaction of surface plasmon polaritons (SPP's) propagating on a metal surface with a sharpened metal tip placed very close to the surface. They excited optically SPP's on a thin Ag film by an attenuated total reflection (ATR) method and detected the modulation of reflected light caused by the tip. They attained 3-nm lateral resolution by scanning the tip. In theoretical treatments of the tip-surface system, the tip is often modeled by a sphere,[12,13] since the exact shape of the tip is not well known. Therefore, a system consisting of a metallic sphere placed very close to a metallic surface provides an important model for discussing the performance of SNOM.

As mentioned above, the metal sphere-surface system is an important system encountered in various optical studies. However, the optical properties of the system have not yet been fully explored. From an experimental point of view, it is rather difficult to prepare stable metallic spherical particles placed very close to a metallic surface. Although Holland and Hall[14] investigated optical properties of a system of Ag-island particles placed on an Ag surface, they did not perform electron microscopic studies of the island particles and, consequently, the shape and size of the particles were unknown. A systematic study, for example, by varying the particle size and/or the distance between the particle and the surface, is still lacking.

Very recently, we have succeeded in preparing spherical Ag particles, several nanometers in diameter, embedded in SiO_2 thin-film matrices (Ag-SiO_2 films) by applying a rf cosputtering technique.[15] Depositing the Ag-SiO_2 thin film on Al surfaces and using the ATR spectroscopy, we studied the change in the SPP dispersion curve caused by the presence of Ag particles on the Al surface.[16] In that work, we could systematically vary the distance between the particles and the surface by inserting thin SiO_2 spacer layers of various thicknesses in between the Al surface and the Ag-SiO_2 film. The SPP dispersion curve was found to depend strongly on the distance between the particle and the surface.

This work is an extension of previous work on the dispersion curve[16] and we report here on light emission from SPP's mediated by Ag particles. It is well known that SPP's on a smooth surface are nonradiative modes and cannot directly emit light.[17] However, in the presence of surface roughness (periodic or random), roughness-mediated light emission becomes possible.[17–20] The purpose of this paper is to experimentally demonstrate that Ag particles placed very close to an Al surface also give rise to strong light emission from SPP's. The intensity of emitted light was found to rapidly decrease as the particle-surface distance increases. The intensity was also found to take a maximum around a wavelength of 520 nm. The experimental results were compared with

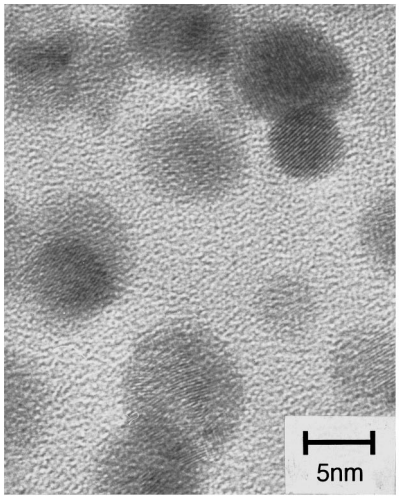

FIG. 1. High-resolution electron micrograph of Ag-SiO_2 composite film prepared by a rf cosputtering method. Dark patches correspond to Ag particles.

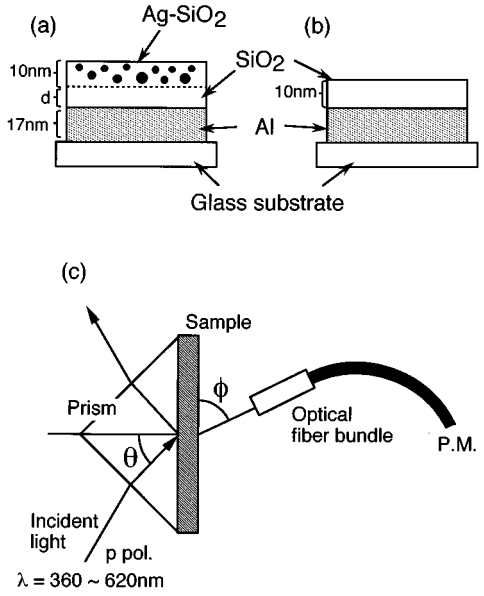

FIG. 2. (a) and (b) Structures of the samples prepared. (c) Experimental arrangement for measurements of light emission under SPP excitation.

theoretical calculations based on a formalism developed by Aravind and Metiu[5] for a metal sphere-surface system. A good qualitative agreement between experimental and theoretical results suggests that the excitation of the gap mode and the surface current associated with the mode play essential roles in the light-emission processes.

II. EXPERIMENTS

Spherical Ag nanoparticles were prepared by a rf cosputtering technique.[15] Small pieces of Ag ($2.5\times15\times2$ mm^3) were placed on a SiO_2 target, 10 cm in diameter, and they were cosputtered in Ar gas of 2.7Pa at a rf power of 50 W by a magnetron sputtering apparatus (Anelva SPF-210H). The filling factor of Ag (the ratio of the volume of Ag to the total volume) was estimated to be 0.05, which was obtained by the density measurements described elsewhere.[21] Figure 1 shows a typical high-resolution transmission electron microscopic (HRTEM) image of the Ag-SiO_2 film. The film deposited onto a cleaved KBr plate was wet stripped and mounted on an electron microscopic grid. The HRTEM image was obtained by an electron microscope (Jeol JEM-2010) operated at 200 kV. In Fig. 1 we can see the dark patches corresponding to Ag particles. Lattice fringes seen in some particles are the {111} planes of Ag crystals. The Ag particles are almost spherical and well dispersed in a SiO_2 matrix. The average diameter estimated from several images was 5.6 nm with a standard deviation of 2.1 nm.

The system of Ag particles placed on Al surface was realized by preparing samples shown in Fig. 2(a). First, Al films, 17 nm thick were evaporated on a glass substrate in a high vacuum of 2×10^{-4} Pa. Spacer layers of SiO_2 were then deposited on the Al film by sputtering the SiO_2 target. Ag-SiO_2 films, 10 nm thick, were finally deposited on top of the spacer layer with the same condition as that prepared for the HRTEM observations. In order to change the distance between the Al surface and the Ag particles, the thickness of the spacer layer (d) was varied from 0 to 9 nm. Hereafter, the samples are labeled by the thickness of the spacer layer. For example, if the spacer layer thickness is 3 nm, the sample is denoted as d-3. For purposes of comparison, a sample whose overlayer did not contain Ag particles was also prepared, as shown in Fig. 2(b). The thicknesses of the deposited layers were monitored by a quartz oscillator calibrated by an optical interference thickness meter (Anelva Nanoscope).

In order to excite SPP's on the Al-overlayer interface, we used an angle-scan ATR method, shown schematically in Fig. 2(c). The sample was pasted onto a right-angle glass prism (BK-7) with the aid of index matching oil, and the prism was mounted on a rotating stage driven by a stepping motor. As a light source, a Xe lamp was used. The light monochromatized by a grating monochromator (Nikon G250) was directed on the sample through the prism. The illuminated spot was about 1×1 mm^2 in size. Since the SPP's are transverse magnetic (TM) modes, the incident light was set to the p polarization with a polarizer. The intensity of reflected light was measured by a Si photodiode (Hamamatsu photonics S1227BR) as a function of the incident angle θ, which is the angle from the normal to the sample surface inside the prism. In order to obtain the ATR spectrum, i.e., θ dependence of the reflectance, raw reflected light intensities were divided by a reference signal, which is the intensity of light reflected by the bare part of the sample. It is known that a larger angular spread of incident light leads to a broader ATR spectrum.[22] To avoid the broadening of the spectrum, appropriate lenses and a pinhole were adopted to minimize the incident beam spread. The angular spread of our configuration was at most 0.2°. Since the widths of measured ATR spectra were much larger than the beam spread, the influence of the beam spread on the present ATR spectra can be neglected.

As shown in Fig. 2(c), the light emitted from the sample was collected by an optical fiber bundle that views the sample and guided to a photomultiplier (Hamamatsu photonics 1P28A). The aperture of the light collection was 2.5 mm in diameter. The distance between the aperture of the fiber

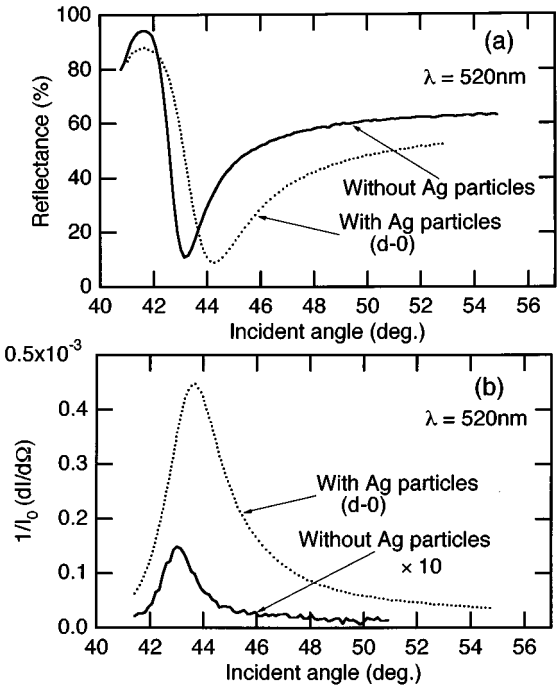

FIG. 3. (a) ATR spectra and (b) θ dependences of emitted light for the sample with (d-0) and without Ag particles. The emitted light was measured fixing the observation angle ϕ at 90°. The wavelength of the incident light was set to 520 nm.

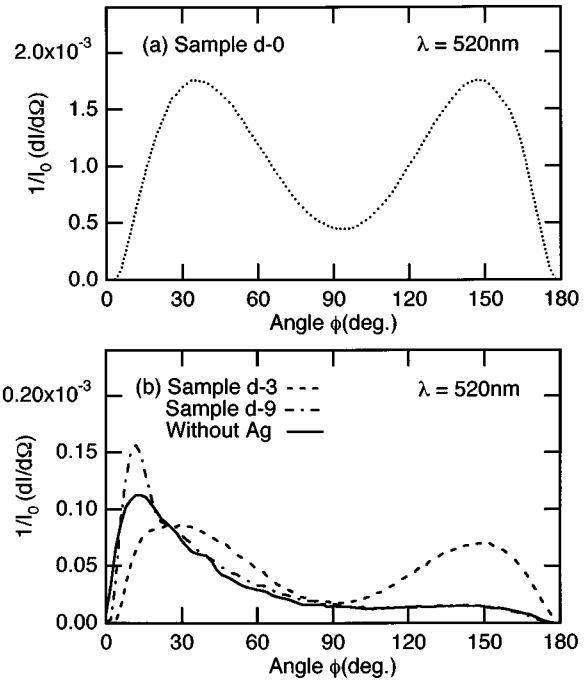

FIG. 4. Angular patterns of emitted light under SPP excitation condition for samples d-0 [dotted line in (a)], d-3 [broken line in (b)], d-9 (dash-dotted line in (b)], and without Ag particle [solid line in (b)]. The incident wavelength was set to 520 nm.

and the sample was 30 mm. The solid angle of the light collection was 5.5×10^{-3} sr, corresponding to the angular resolution of 4.8°. The light intensity was measured with a chopper and a lock-in amplifier (NF LI-570). We performed two types of measurements. In one type of measurement the light intensity was measured as a function of the incident angle θ, fixing the observation angle ϕ at 90° (θ-scan emission spectrum). From the θ-scan emission spectrum, we can confirm the excitation of SPP since the emission intensity takes a maximum at a SPP-excitation angle θ_{SPP}. In the other type of measurement the light intensity was measured as a function of ϕ, fixing the incident angle at θ_{SPP}. From this measurement we obtained the angular pattern of the light emitted from the excited SPP. The above experiments were performed for various incident wavelengths (λ=350–620 nm).

III. RESULTS

Figure 3 shows typical (a) ATR and (b) θ-scan emission spectra obtained for the sample d-0 and the sample without Ag particles. The incident wavelength (λ) was 520 nm. The ordinate in Fig. 3(b) represents the light intensity per unit solid angle normalized to the intensity of the incident light. The ATR spectra show a dip in reflectance due to the resonant excitation of the SPP on Al-overlayer interface. The existence of Ag fine particles is found to cause a shift of the ATR dip to higher angles and makes the dip broad, in good agreement with our previous detailed ATR results.[16] In the emission spectra, we find a peak located at almost the same angle as the ATR dip. The agreement between the ATR dip positions and the peak positions of the emission spectra implies that the light emission is due to the radiative decay of the SPP into the air side. The weak emission peak observed for the sample without Ag particles is attributed to the radiative decay of the SPP mediated by the surface roughness at the Al-SiO_2 interface. It should be stressed that the peak intensity of the sample d-0 is about one order of magnitude larger than that of the sample without Ag particles. Figure 3(b) demonstrates that the presence of the Ag particles gives rise to the strong light emission of the SPP.

Figures 4(a) and 4(b) show the ϕ dependences of the emission intensity, i.e., the angular patterns of light emitted from the SPP. The SPP was excited with λ=520 nm. The data obtained for the sample d-0 are presented in Fig. 4(a) and the data for the samples d-3, d-9, and without Ag particles are shown in Fig. 4(b). The angular pattern obtained for the sample without Ag particles exhibits a lobe around ϕ=10°. This pattern is similar to those reported for nominally smooth (slightly roughened) metallic surfaces.[20] For a thick spacer layer (sample d-9), the angular pattern is almost the same as that for the sample without Ag particles. As d decreases, the lobe observed around 10° decreases, while the two lobes around 30° and 150° grow. The intensities of the lobes increase drastically with decreasing d from 3 to 0 nm. This indicates that the Ag particles placed within the diameter (about 5 nm) from the Al surface strongly contribute to the light emission from the SPP.

To gain insight into the mechanism of the strong light emission mediated by Ag particles, the measurement of the angular pattern was performed for various λ in the range 350–620 nm. Figure 5 shows the λ dependences of the emitted light intensity. In this figure, the light intensity integrated over ϕ is plotted. We see that the sample d-9 emits light with almost the same intensity as the sample without Ag particles. As d decreases, the emitted light intensity drasti-

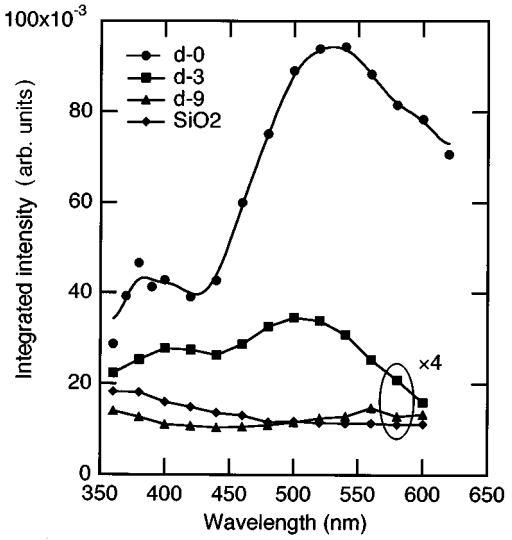

FIG. 5. Wavelength dependences of emitted light intensity under SPP excitation. The intensity was integrated from $\phi=0$ to 180°. Obtained data were corrected by the wavelength dependence of the incident light intensity.

cally increases. The dramatic increase is again found between $d=3$ and 0 nm. The most interesting feature in this figure is a large peak observed around $\lambda=520$ nm in the case of no spacer layer, i.e., for sample d-0.

IV. COMPARISON WITH CALCULATION AND DISCUSSION

It is well known that an isolated metal fine particle supports resonance modes of plasma oscillation of free electrons, so-called localized surface plasmons (LSP's). The resonance frequencies of LSP's in a metal sphere are determined by $\epsilon(\omega)=-\epsilon_m(n+1)/n$, where n is an integer and $\epsilon(\omega)$ and ϵ_m are the dielectric functions of the metal and the surrounding medium, respectively.[23] For a sphere much smaller than the wavelength of the incident light, only the LSP mode of $n=1$ is excited. Aravind and Metiu[5] calculated the optical response of a metal particle-surface system, in which a metallic particle is placed very close to a metallic flat surface. They showed that a number of resonances exist in the frequency region lower than that of the LSP mode of $n=1$. These resonances correspond to electromagnetic normal modes of the particle-surface system generated by the coupling of the LSP modes with their image charges. The electric fields associated with these normal modes are highly localized at the particle-surface gap and thus they are called ''gap modes.''

For our samples, in particular with thin spacer layers, the gap modes are believed to play important roles in the light emission processes. Since the resonance wavelength of the LSP in isolated Ag particles in SiO_2 is located at 410 nm,[16] the resonances of the gap modes in our samples are expected to lie in a wavelength region longer than 410 nm. As seen in Fig. 5, the peak of emitted light intensity observed for the sample d-0 is located around 520 nm, suggesting strongly the contribution of the gap modes.

We propose here the following processes for the light emission from SPP mediated by metallic particles: (i) The SPP at the Al-overlayer interface is first excited optically by the ATR method, (ii) the electromagnetic fields associated with the SPP then excite the gap mode of the Ag particle-Al surface system, (iii) the surface current on the Al surface is induced upon excitation of the gap mode, and finally (iv) the surface current emits light. On the basis of the above scenario, we performed electromagnetic calculations and attempted to theoretically reproduce the observed characteristics of the light emission. In the following subsections, formalisms of the calculations corresponding to processes (i)–(iv) are described and results of numerical calculation are compared with experimental ones.

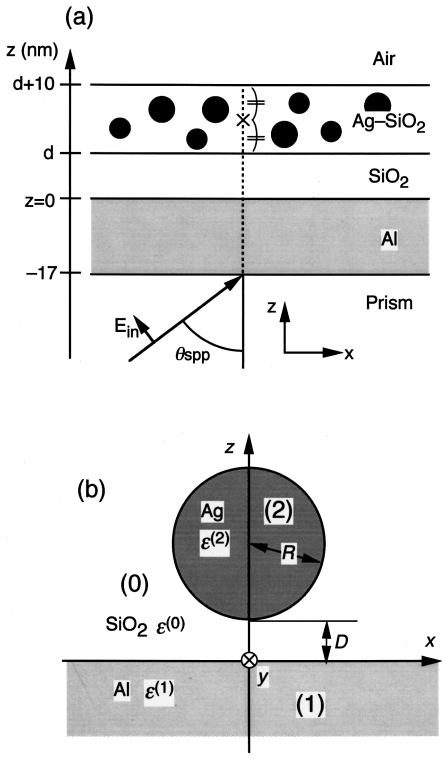

FIG. 6. (a) Multilayered structure assumed to calculate the electric field associated with SPP. The Ag-SiO_2 film is regarded as an effective medium, which has an averaged dielectric constant ϵ_{av} calculated by Maxwell-Garnett theory. (b) Ag particle–Al surface system considered in calculation. An Ag spherical particle of radius R is placed at a distance D above Al-SiO_2 interface. The center of the sphere is on the z axis, and the x-y plane corresponds to the Al-SiO_2 interface.

A. SPP field in the Ag-SiO_2 composite layer

In this subsection we calculate the electric field in the Ag-SiO_2 associated with the SPP excited by the ATR method. We consider a multilayered structure (prism/Al/SiO_2/Ag-SiO_2/air) shown in Fig. 6(a). The incident light is assumed to be a p-polarized plane wave with an electric field amplitude of E_{in}. Using a 2×2 transfer matrix method,[24] we can calculate the electric field for a given incident angle θ and angular frequency ω at any position specified by the coordinate z. In actual computations, we need values of the dielectric constants for all layers. The values

for Al (Ref. 25) and SiO_2 (Ref. 26) were taken from literature. The Ag-SiO_2 was regarded as an effective medium and its dielectric constant was calculated in a manner described elsewhere,[27] which is based on the effective-medium theory developed by Maxwell-Garnett.[28] In calculating the effective dielectric constants, we used the dielectric constants of the Ag nanoparticle, which were obtained from the bulk value[29] by taking into account the reduction of the mean free path of free electrons due to the scattering at particle surfaces.[30] The filling factor of Ag was set to 0.05, which is estimated by density measurements for the present film. The thicknesses of the Al and Ag-SiO_2 layers were set to the experimental values of 17 and 10 nm, respectively. The SiO_2 spacer thickness d was varied from 0 to 9 nm.

We calculated the electric field at the center of the Ag-SiO_2 layer by varying the incident angle θ. The field intensity exhibited a pronounced peak at a certain angle θ_{SPP}, which corresponds to the excitation of the SPP. At $\theta=\theta_{\mathrm{SPP}}$, we also calculated the field distribution in the multilayer system. The SPP-field intensity was found to take a maximum at the Al-SiO_2 interface and decay away from the interface. In the Ag-SiO_2 layer, however, the field intensity was almost constant because the field decay length (several hundred nanometers) is much larger than the Ag-SiO_2 thickness. Therefore, it suffices to use the electric field calculated at the center of the Ag-SiO_2 layer, $\mathbf{E}(\theta_{\mathrm{SPP}},\omega)_{z=d+5\,\mathrm{nm}}$, as the driving field of the gap mode.

The SPP field in the Ag-SiO_2 layer, $\mathbf{E}(\theta_{\mathrm{SPP}},\omega)_{z=d+5\,\mathrm{nm}} \equiv \mathbf{E}_{\mathrm{SPP}}(\omega)$, was calculated for various wavelengths and spacer thicknesses corresponding to the present experiments. The calculated $\mathbf{E}_{\mathrm{SPP}}(\omega)$ was found to be almost independent of the spacer thickness d. This is because the $1/e$ field decay length is several hundred nanometers, which is much lager than the spacer layer thickness.

B. Local field associated with the gap mode

The SPP field will excite the gap modes, giving rise to strong electromagnetic fields localized in spaces between the Ag particles and Al surface. In this subsection we calculate the local electric field associated with the gap modes. Although the actual samples consist of many particles, for simplicity we consider here a single particle placed near a flat surface, as shown in Fig. 6(b). This simplification is allowed for our samples since the distances between the particles are large enough to neglect the electromagnetic interactions between the particles. An Ag sphere of radius R is assumed to be placed at a distance D above an Al surface. For convenience, we assume that the center of the sphere is above the origin, i.e., on the z axis, and the Al-SiO_2 interface is expressed by $z=0$ (the x-y plane). The regions (0), (1), and (2) correspond to SiO_2, Al, and Ag, respectively. Because both D and R are much smaller than the wavelength of SPP ($2\pi/k_{\mathrm{SPP}}$), which is of the order of 100 nm, we can neglect the retardation. For the case where an external electric field $\mathbf{E}^{\mathrm{ex}(0)}$ with a constant amplitude is applied in the region (0), the local field induced around the sphere can be calculated by a method developed by Aravind and Metiu.[5] In the nonretardation limit, the problem reduces to solving Laplace's equation in the particle-surface system. The potentials expressed in the bispherical coordinates μ, η, and φ, take the form,[5,31]

$$\Phi^{(0)}(\mu,\eta,\varphi)=F\sum_{n\geqslant|m|}^{\infty}\sum_{m=-\infty}^{+\infty}[A_n^m e^{(n+1/2)\mu} + B_n^m e^{-(n+1/2)\mu}]Y_n^m(\cos\eta,\varphi)-\mathbf{E}^{\mathrm{ex}(0)}\mathbf{r}, \tag{1a}$$

$$\Phi^{(1)}(\mu,\eta,\varphi)=F\sum_{n\geqslant|m|}^{\infty}\sum_{m=-\infty}^{+\infty}D_n^m e^{(n+1/2)\mu}Y_n^m(\cos\eta,\varphi) - \mathbf{E}^{\mathrm{ex}(1)}\mathbf{r}, \tag{1b}$$

$$\Phi^{(2)}(\mu,\eta,\varphi)=F\sum_{n\geqslant|m|}^{\infty}\sum_{m=-\infty}^{+\infty}C_n^m e^{-(n+1/2)\mu}Y_n^m(\cos\eta,\varphi), \tag{1c}$$

where $\Phi^{(0)}$, $\Phi^{(1)}$, and $\Phi^{(2)}$ are the potentials in SiO_2, Al, and Ag, respectively, and A_n^m, B_n^m, C_n^m, and D_n^m are expansion coefficients. The definition of the spherical harmonics $Y_n^m(\cos\eta,\varphi)$ is the same as in Ref. 31 and $F\equiv(\cosh\mu-\cos\eta)^{1/2}$. The term $\mathbf{E}^{\mathrm{ex}(1)}$ in Eq. (1b) is a mathematical artifact that is introduced by following the previous theoretical treatment.[5] This term is related to $\mathbf{E}^{\mathrm{ex}(0)}$ by the boundary conditions at the Al-SiO_2 interface and is identical to the electric field in Al layer calculated in the absence of Ag particle. In the bispherical coordinates, the Al surface (x-y plane) coincides with $\mu=0$ and the surface of the sphere is given by $\mu=\mu_0$, with

$$\mu_0=\mathrm{arccosh}(1+D/R). \tag{2}$$

We apply the following boundary conditions to Eqs. (1a), (1b), and (1c):

$$\Phi^{(0)}(\mu=0^+,\eta,\varphi)=\Phi^{(1)}(\mu=0^-,\eta,\varphi), \tag{3a}$$

$$\Phi^{(0)}(\mu=\mu_0^+,\eta,\varphi)=\Phi^{(2)}(\mu=\mu_0^-,\eta,\varphi), \tag{3b}$$

$$\epsilon^{(0)}\frac{\partial\Phi^{(0)}}{\partial\mu}(\mu=0^+,\eta,\varphi)=\epsilon^{(1)}\frac{\partial\Phi^{(1)}}{\partial\mu}(\mu=0^-,\eta,\varphi), \tag{3c}$$

$$\epsilon^{(0)}\frac{\partial\Phi^{(0)}}{\partial\mu}(\mu=\mu_0^+,\eta,\varphi)=\epsilon^{(2)}\frac{\partial\Phi^{(2)}}{\partial\mu}(\mu=\mu_0^-,\eta,\varphi), \tag{3d}$$

and then obtain the equations for the expansion coefficients A_n^m, B_n^m, C_n^m, and D_n^m. The equations can be solved by following Ref. 5. The electric field can be obtained from $\mathbf{E}=-\mathrm{grad}\Phi$ in the bispherical coordinates as,[5]

$$E_\nu=-\frac{1}{h_\nu}\frac{\partial\Phi}{\partial\nu}, \tag{4}$$

with $\nu=\mu$, η, or φ; $h_\mu=h_\eta=c(\cosh\mu-\cos\eta)^{-1}$; $h_\varphi=c\sin\eta(\cosh\mu-\cos\eta)^{-1}$; and $c=R[(1+D/R)^2-1]^{1/2}$.

In order to calculate the local electric field induced under SPP excitation, the external field $\mathbf{E}^{\mathrm{ex}(0)}$ in Eq. (1a) is now taken to be the electric field of SPP ($\mathbf{E}_{\mathrm{SPP}}$) calculated in Sec.

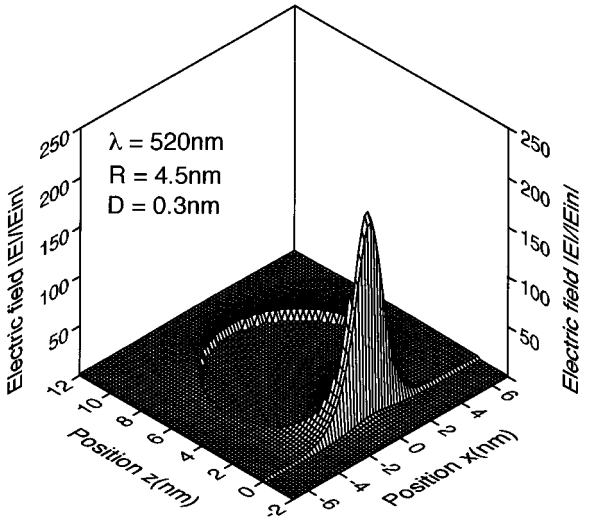

FIG. 7. Calculated spatial distribution of electric-field intensity around an Ag sphere under SPP excitation. The absolute value of the electric field normalized to the amplitude of incident field E_{in} in Fig. 5(a) is shown as a function of the position in x-z plane. The incident wavelength was set to 520 nm. R and D are assumed to be 4.5 and 0.3 nm, respectively.

IV A. Since the SPP is a TM mode, $\mathbf{E}_{\mathrm{SPP}}$ has the x and z components. We calculated numerically the local electric fields $\mathbf{E}^{(0)}$, $\mathbf{E}^{(1)}$, and $\mathbf{E}^{(2)}$ in regions of SiO_2, Al, and Ag, respectively. The radius R of the Ag sphere was fixed at 4.5 nm throughout the present calculations. The reason why R was fixed will be discussed later.

Figure 7 shows the spatial distribution of the local electric field around the Ag sphere upon SPP excitation. The value of $\mathbf{E}_{\mathrm{SPP}}$ calculated for the sample d-0 was used as $\mathbf{E}^{\mathrm{ex}(0)}$ in this calculation. R, D, and λ were set to 4.5, 0.3, and 520 nm, respectively. In this figure, the absolute value of $\mathbf{E}$ normalized to the amplitude of the incident-light field E_{in} defined in Fig. 6(a) is plotted as a function of the position in x-z plane. The Ag sphere corresponds to a circle of radius 4.5 nm with the center located at $z=4.8$ nm and $x=0$ nm, and the Al layer corresponds to the region of $z\leqslant 0$. In Fig. 7 we see that the electric fields inside the metals (Ag particle and Al) are almost constant and very small. Just outside the metals, the strong field is induced. In particular, at the particle-surface gap, the electric field is highly enhanced, demonstrating that the gap mode is excited.

We also calculated the electric field for the case of $D=3$ nm corresponding to the sample d-3. In that calculation, R was set to 4.5 nm and the value of $\mathbf{E}_{\mathrm{SPP}}$ calculated for the sample d-3 was used as $\mathbf{E}^{\mathrm{ex}(0)}$. The calculated field intensity almost coincided with that obtained for $D=0.3$ nm, except for the region of the gap. In the gap region, however, the value of $|\mathbf{E}|/E_{\mathrm{in}}$ was smaller than that for $D=0.3$ nm by almost an order of magnitude.

C. Surface current induced on Al surface

As seen in Fig. 7, a large discontinuity of the electric field is found at the Al-SiO_2 interface, suggesting that a large amount of surface charge is induced at the interface. Since the electric field is assumed implicitly to oscillate with the frequency ω of SPP, the surface charge also fluctuates with ω. The fluctuation of the surface charge is expected to become a radiation source. To describe the motion of the surface charge, we introduce here the surface current, which is obtained by the difference of the polarization currents at the surface.[18,19] The surface current on the Al surface is given by

$$\mathbf{J}(\mathbf{r},\omega)=\left[\frac{(\epsilon^{(0)}-1)}{4\pi}\frac{\partial}{\partial t}\mathbf{E}^{(0)}(\mathbf{r},\omega)\right]_{z=+0}-\left[\frac{(\epsilon^{(1)}-1)}{4\pi}\frac{\partial}{\partial t}\mathbf{E}^{(1)}(\mathbf{r},\omega)\right]_{z=-0}, \tag{5}$$

where $\mathbf{E}^{(0)}(\mathbf{r},\omega)$ and $\mathbf{E}^{(1)}(\mathbf{r},\omega)$ are the local electric fields calculated in the SiO_2 and Al regions, respectively, and $\mathbf{r}$ moves on the x-y plane. From $\mathbf{E}^{(0)}(\mathbf{r},\omega)=\mathbf{E}^{(0)}(\mathbf{r})e^{-i\omega t}$ and $\mathbf{E}^{(1)}(\mathbf{r},\omega)=\mathbf{E}^{(1)}(\mathbf{r})e^{-i\omega t}$, the above equation becomes

$$\mathbf{J}(\mathbf{r},\omega)=\left[\frac{-i\omega(\epsilon^{(0)}-1)}{4\pi}\mathbf{E}^{(0)}(\mathbf{r},\omega)\right]_{z=+0}-\left[\frac{-i\omega(\epsilon^{(1)}-1)}{4\pi}\mathbf{E}^{(1)}(\mathbf{r},\omega)\right]_{z=-0}. \tag{6}$$

In previous studies on the light emission of SPP via the surface roughness, Kröger and Kretshmann[18] demonstrated that the surface current generated by the roughness acts as a radiation source. In their calculation, the radiation source was assumed to be the difference of the surface currents in the presence and absence of the roughness. In the present study, we assume the radiation source to be the difference of the surface currents in the presence and absence of the Ag particle. The radiation source is then given by

$$\mathbf{J}(\mathbf{r},\omega)=\left[\frac{-i\omega(\epsilon^{(0)}-1)}{4\pi}\mathbf{E}^{(0)}(\mathbf{r},\omega)\right]_{z=+0}-\left[\frac{-i\omega(\epsilon^{(1)}-1)}{4\pi}\mathbf{E}^{(1)}(\mathbf{r},\omega)\right]_{z=-0}-\left\{\left[\frac{-i\omega(\epsilon^{(0)}-1)}{4\pi}\mathbf{E}^{\mathrm{ex}(0)}(\mathbf{r},\omega)\right]_{z=+0}-\left[\frac{-i\omega(\epsilon^{(1)}-1)}{4\pi}\mathbf{E}^{\mathrm{ex}(1)}(\mathbf{r},\omega)\right]_{z=-0}\right\}, \tag{7}$$

where $\mathbf{E}^{\mathrm{ex}(0)}$ and $\mathbf{E}^{\mathrm{ex}(1)}$, which are identical to those in Eq. (1), are the external fields in the regions (0) and (1), respectively, in the absence of the Ag particle. To obtain Cartesian coordinate components J_x, J_y, and J_z, the $\mathbf{E}^{(n)}(n=0,1)$ expressed in bispherical coordinates were transformed to those in Cartesian coordinates through

$$E_x(\mathbf{r})=-E_\varphi(\mathbf{r})\sin\varphi-E_\eta(\mathbf{r})\cos\varphi, \tag{8a}$$

$$E_y(\mathbf{r})=E_\varphi(\mathbf{r})\cos\varphi-E_\eta(\mathbf{r})\sin\varphi, \tag{8b}$$

$$E_z(\mathbf{r})=E_\mu(\mathbf{r}). \tag{8c}$$

These hold at $z=0$ (on x-y plane).

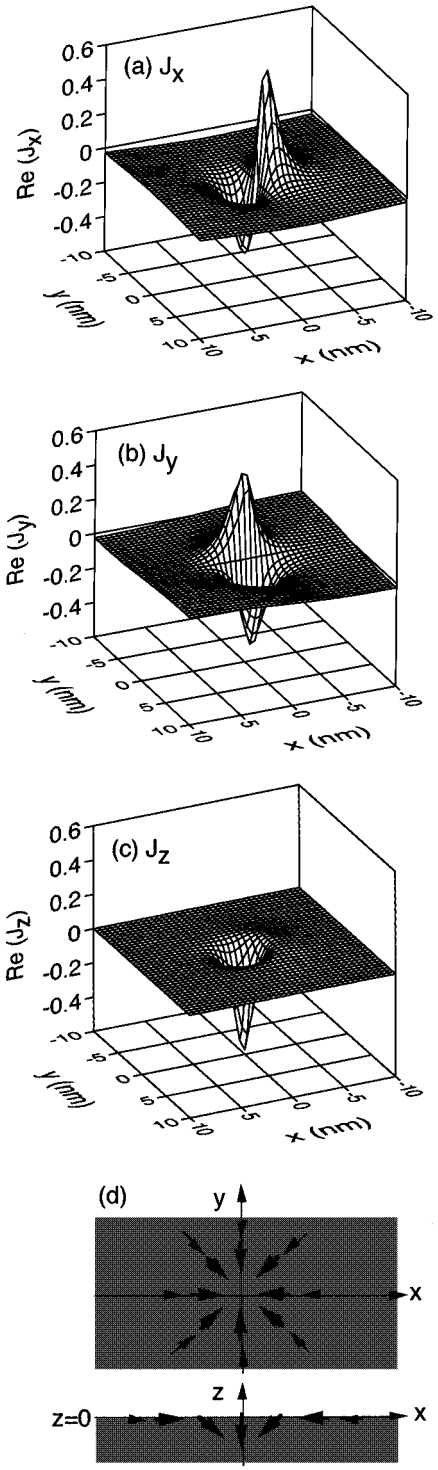

FIG. 8. Calculated profiles of surface current induced on the Al surface (x-y plane) under the same condition as in Fig. 6 ($\lambda=520$ nm, $R=4.5$ nm, and $D=0.3$ nm). (a), (b), and (c) represent real parts of x, y, and z components of the surface current, respectively. (d) schematically shows the motion of the surface charge predicted by (a)–(c).

Using Eq. (7), we numerically calculated the surface current induced by the existence of the Ag particle. The parameters used in the calculation ($R=4.5$ nm, $D=0.3$ nm, and $\lambda=520$ nm) are the same as those used to obtain the result in Fig. 7. Figures 8(a)–8(c) illustrate profiles of the surface current ($\mathbf{J}$) on the x-y plane (on the Al surface). In the Figs. 8(a), 8(b), and 8(c) the real parts of J_x, J_y, and J_z are shown, respectively. Figure 8(d) schematically shows the motion of the charges predicted by the profiles of J_x, J_y, and J_z. As seen in Figs. 8(a)–8(c), the surface current induced by the gap mode is highly localized around $x=y=0$, i.e., just beneath the center of the Ag particle, and concentrated within a projected area of the Ag particle.

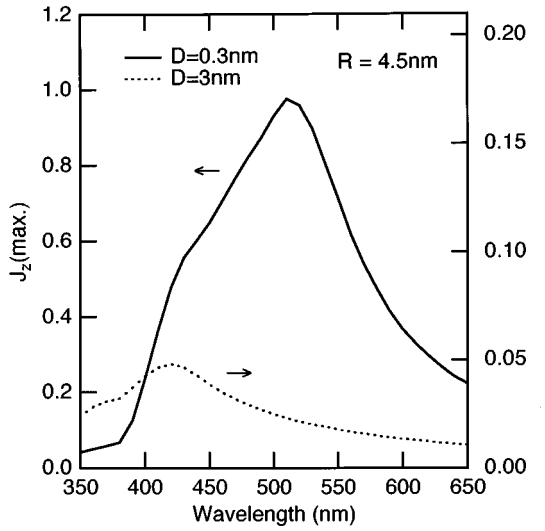

FIG. 9. Calculated wavelength dependences of z component of surface current J_z induced on the Al surface under SPP excitation. The plotted data are the maximum values of the amplitude. Solid and dashed lines correspond to $D=0.3$ and 3 nm, respectively.

We see that, in the profiles of J_x and J_y, there are two poles with opposite signs. For J_y, the magnitudes of the poles are identical to each other and there is a point symmetry about the origin. On the other hand, the J_x profile is found to be slightly asymmetric, arising from the asymmetry of the applied field, which has not only the z component but also a small-x component. Since, however, the asymmetry in J_x is small enough to be negligible, we can regard the parallel component of $\mathbf{J}$ [$\mathbf{J}_\parallel \equiv (J_x, J_y, 0)$] as symmetric about the origin, as is illustrated in the upper side of Fig. 8(d). This means that $\mathbf{J}_\parallel(\mathbf{r})$ and $\mathbf{J}_\parallel(-\mathbf{r})$ have the same magnitude, but there is a phase difference of π between them. Therefore, the far field radiated from $\mathbf{J}_\parallel(\mathbf{r})$ is canceled out by that from $\mathbf{J}_\parallel(-\mathbf{r})$ due to the destructive interference. On the contrary, for J_z, the cancellation does not occur as is expected by the profile [Fig. 8(c)]. Therefore, J_z can contribute to the light emission.

The current profiles were calculated for various excitation wavelengths. Figure 9 indicates λ dependences of J_z. In this figure, maximum values in the calculated profiles of J_z are plotted. Solid and dashed lines correspond to $D=0.3$ and 3 nm, respectively. The radius R was again set to 4.5 nm. For $D=0.3$ nm, we see a pronounced peak around 520 nm. The peak corresponds to the excitation of the gap mode. On the other hand, for $D=3$ nm the peak is very weak and is located around 420 nm, which is almost the same as the resonance wavelength of the LSP in the isolated Ag particle in SiO_2. It should be noted here that the peak position for $D=0.3$ nm agrees well with that of the emitted light intensity observed

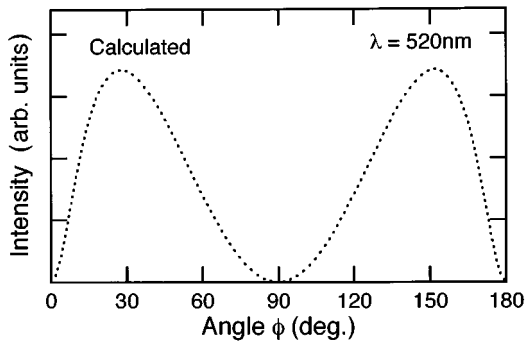

FIG. 10. Calculated angular pattern of light emission yielded by a current source that is assumed to have only a z component and to be a δ function. The point source is assumed to be positioned in the center of a vacuum thin layer, 0.1 nm in thickness, which was added in the structure of the sample d-0, yielding a multilayer of air/Ag-SiO_2/vacuum/Al/prism.

for the sample d-0 (closed circles in Fig. 5). Moreover, the calculated J_z dramatically decreases with increasing D, which agrees fairly well with the drastic decrease in the light intensity observed with increasing d (Fig. 5).

D. Radiation pattern generated by J_z

In an attempt to explain the radiation pattern obtained experimentally [Fig. 4(a)], we calculated the angular pattern of light emitted from J_z. Since J_z is highly localized as seen in Fig. 8(c), J_z can be approximately described using a δ function. We consider here the radiation pattern from a point current source $\mathbf{J}=(0,0,\delta(\mathbf{r}))$ located on the Al surface. The intensity of light emitted from a point source can be calculated from the electromagnetic Green's function. We followed a manner previously described by Reed *et al.*[24] for a current source positioned in a multilayer system. The point source was positioned in a vacuum thin layer, which was added in the structure of the sample d-0, yielding the multilayer of air/Ag-SiO_2/vacuum/Al/prism. The vacuum thin layer to locate the radiation source was proposed by Kröger and Kretschmann[18] in their study on the roughness-mediated SPP radiation. We assumed the thickness of the vacuum layer to be 0.1 nm and placed the point source at the center of the layer.

Figure 10 shows the angular pattern of the light emitted into the air side. The calculated angular pattern has two lobes around 30° and 150°, in good agreement with the experimental result for the sample d-0 [Fig. 4(a)]. We can conclude that the light emission in the experiment is dominated by the z component of the localized surface current. From a close comparison of Fig. 4(a) with Fig. 10, however, we find that the calculated pattern slightly differs from the experimental one around $\phi=90°$. In the experimental result [Fig. 4(a)], the emitted light does not vanish at $\phi=90°$. This is because the x component of the surface current is not taken into account in the angular pattern calculation. As was stated earlier, the J_x profile is slightly asymmetric [Fig. 8(a)]. This means that the field radiated from $J_x(\mathbf{r})$ is not completely canceled out by that from $J_x(-\mathbf{r})$. The far field remains after the destructive interference. The parallel component of the current source on a metal is known to lead a broad lobe at $\phi=90°$ in the angular pattern.[32] Therefore, the light observed around $\phi=90°$ is believed to arise from J_x.

E. Discussion

As can be seen in Fig. 7, the surface charge is induced not only on the Al surface but also on the Ag particle. The surface charge fluctuation on the Ag particle may also contribute to the light emission. It is known that the surface charge induced on a sphere produces an electric dipole $\mathbf{p}$, which is given by[33]

$$\mathbf{p}(\omega)=\int_{\text{sphere}}\mathbf{r}\sigma(\mathbf{r},\omega)ds, \tag{9}$$

where σ is the surface charge density on the Ag particle and $\mathbf{r}$ moves on the spherical surface. For the present particle-surface system [Fig. 6(b)], we calculated the electric-dipole moment of the Ag particle for various D. The actual calculation in the bispherical coordinates was carried out following the method described by Goyette and Navon.[33] The magnitude of the calculated dipole moment $|\mathbf{p}(\omega)|$ was found to depend very weakly on D. The calculated $|\mathbf{p}(\omega)|$ for $D=9$ nm had the same order of magnitude as that for $D=0.3$ nm. In contrast, the emitted light observed experimentally for the sample d-9 is very much weaker than that for the sample d-0. Therefore, the light emission observed cannot be explained by the radiation from the electric dipole induced on the Ag particles.

Although there exist distributions of the radius R and distance D of Ag particles contained in the Ag-SiO_2 layer prepared, the experimental results (Fig. 5) could be explained well by the calculation (Fig. 9) with the fixed R (4.5 nm) and D (0.3 nm). The reason for this may be argued as follows. As seen in Fig. 8(c), the localization area of J_z is of the order of R^2. On the other hand, the maximum value in J_z is proportional to $(D/R)^{-1}$. The total amount of J_z (J_{total}) is roughly proportional to the product of the localization area and the maximum value, i.e., $R^2(D/R)^{-1}$. As a consequence, the emitted light power ($\propto J_{\text{total}}^2$) is proportional to $[R^2(D/R)^{-1}]^2=R^6D^{-2}$. This means that the Ag particles with large R and small D dominate the light emission. In the present Ag-SiO_2 layer, the mean radius of the Ag particles was about 3 nm. As seen in the present TEM image (Fig. 1), however, large Ag particles 4–5 nm in radius are also contained in a certain proportion (about 10% in number). In the present sample, the large Ag particles 4–5 nm in radius located very close to the Al surface are thus thought to dominantly contribute to the light emission.

V. CONCLUSION

We investigated the light emission from SPP's mediated by metallic nanoparticles. A system consisting of Ag nanoparticles placed very close to an Al surface was prepared by depositing a Ag-SiO_2 film on an Al film. The distance between the particles and the surface was systematically changed by varying the thickness of a SiO_2 spacer layer sandwiched between Al and Ag-SiO_2 layers. The SPP on the Al surface was optically excited by means of an ATR method and the light emission from the sample was measured for various excitation wavelengths (λ). The emitted-

light intensity was found to increase rapidly as the particle-surface distance decreases. When the particle-surface distance is less than a few nanometers, i.e., the order of the particle radius, very strong light emission was observed. The emitted-light intensity was also found to vary sensitively with λ and exhibit a maximum around $\lambda = 520$ nm. To clarify the light emission mechanism, we performed electromagnetic calculations and compared the calculated results with experimental ones. From a good qualitative agreement between the experimental and calculated results, we suggested the following processes of the light emission: (i) The SPP's excite electromagnetic normal modes localized in between the Ag particles and the Al surface (gap modes), (ii) localized surface current associated with the gap modes is induced on the Al surface, and (iii) the induced surface current emits light.

The excitation of the gap mode resulting from the interaction of the SPP with a metallic particle induces a very strong electric field in between the particle and surface, which will give rise to various enhancement phenomena. A simple possible experiment is to enhance Raman scattering from molecules or very thin films, which are located between the metallic particles and metallic surface. Due to the strong field of the gap mode, Raman dipoles with large magnitudes will be induced. Attempts to enhance the Raman signal by the gap mode are currently in progress in our laboratory. Such an enhancement will also be observed in other optical processes, e.g., optical absorption, luminescence, and various non-linear optical processes. The combination of the optical enhancement mediated by the gap mode with scanning probe microscopes is an intriguing challenge. For example, a metallic particle attached to a sharpened fiber tip and a fiber tip coated with the metal-particle layer (such as the present Ag-SiO_2 film) seem to be suitable for the probe. In such types of optical scanning probe microscopes, the optical signals only from the tip front are thought to be enhanced and detected, which allows us to perform not only topographic but also spectroscopic investigations of small structures.

ACKNOWLEDGMENT

This work was supported by a Grant-in-Aid for Scientific Research from the Ministry of Education, Science, Sports and Culture, Japan.

*Author to whom correspondence should be addressed. Electronic address: hayashi@eedept.kobe-u.ac.jp

[1] S. L. McCarthy and J. Lambe, Appl. Phys. Lett. **33**, 858 (1978).
[2] R. W. Rendell, D. J. Scalapino, and B. Mühlschlegel, Phys. Rev. Lett. **41**, 1746 (1978).
[3] R. W. Rendell and D. J. Scalapino, Phys. Rev. B **24**, 3276 (1981).
[4] R. Ruppin, Surf. Sci. **127**, 108 (1983).
[5] P. K. Aravind and H. Metiu, Surf. Sci. **124**, 506 (1983).
[6] J. K. Gimzewski, B. Reihl, J. H. Coombs, and R. R. Schlitter, Z. Phys. B **72**, 497 (1988).
[7] R. Berndt, J. K. Gimzewski, and P. Johansson, Phys. Rev. Lett. **67**, 3796 (1991).
[8] P. Johansson and R. Monreal, Z. Phys. B **84**, 269 (1991).
[9] P. Johansson, R. Monreal, and P. Apell, Phys. Rev. B **42**, 9210 (1990).
[10] W. Denk and D. W. Pohl, J. Vac. Sci. Technol. B **9**, 510 (1991).
[11] M. Specht, J. D. Pedarnig, W. M. Heckl, and T. W. Häncsh, Phys. Rev. Lett. **68**, 476 (1992).
[12] A. Madrazo, M. Neito-Vesperinas, and N. García, Phys. Rev. B **53**, 3654 (1996).
[13] M. Neito-Vesperinas and A. Madrazo, in *Photons and Local Probes*, edited by O. Mari and R. Möller (Kluwer Academic, Dordrecht, 1995), p. 35.
[14] W. R. Holland and D. G. Hall, Phys. Rev. B **27**, 7765 (1983).
[15] M. Fujii, T. Nagareda, S. Hayashi, and K. Yamamoto, Phys. Rev. B **44**, 6243 (1991).
[16] T. Kume, N. Nakagawa, S. Hayashi, and K. Yamamoto, Solid State Commun. **93**, 171 (1995).
[17] H. Raether, *Surface Plasmons on Smooth and Rough Surfaces and on Gratings* (Springer, Berlin, 1988).
[18] E. Kröger and E. Kretschmann, Z. Phys. **237**, 1 (1970).
[19] J. Vlieger and D. Bedeaux, Physica A **85**, 389 (1976).
[20] D.-L. Hornauer, Opt. Commun. **16**, 76 (1976).
[21] T. Kume, T. Amano, S. Hayashi, and K. Yamamoto, Thin Solid Films **264**, 115 (1995).
[22] M. Fukui, S. Tago, and K. Oda, J. Phys. Soc. Jpn. **55**, 973 (1986).
[23] R. Ruppin, in *Electromagnetic Surface Mode*, edited by A. D. Boardman (Wiley, Chichester, 1982), p. 345.
[24] C. E. Reed, J. Giergiel, J. C. Hemminger, and S. Ushioda, Phys. Rev. B **36**, 4990 (1987).
[25] D. Y. Smith, E. Shiles, and M. Inokuti, in *Handbook of Optical Constants of Solids*, edited by E. D. Palik (Academic, Orlando, 1985), p. 398.
[26] H. R. Philipp, in *Handbook of Optical Constants of Solids* (Ref. 25), p. 749.
[27] T. Kume, N. Nakagawa, S. Hayashi, and K. Yamamoto, Superlatt. Microstruct. **15**, 459 (1994).
[28] J. C. Maxwell-Garnett, Philos. Trans. R. Soc. London Ser. A **203**, 358 (1904); **205**, 237 (1906).
[29] D. W. Lynch and W. R. Hunter, in *Handbook of Optical Constants of Solids* (Ref. 25), p. 350.
[30] U. Kreibig and C. V. Fragstein, Z. Phys. **224**, 307 (1969).
[31] P.M. Morse and H. Feshbach, *Method of Theoretical Physics* (McGraw-Hill, New York, 1953).
[32] R. G. Greenler, Surf. Sci. **69**, 647 (1977).
[33] A. Goyette and A. Navon, Phys. Rev. B **13**, 4320 (1976).